Structural and Conformational Studies of Diastereoselected Bis(phosphino)amines

Timothy R. Prout, Tomasz W. Imiolczyk, Francoise Barthelemy, Susan M. Young, R. Curtis Haltiwanger, and Arlan D. Norman*

Department of Chemistry and Biochemistry, University of Colorado, Boulder, Colorado 80309

Received November 5, 1993®

Skeletal P–N–P unit conformational preferences of the unsymmetrically substituted bis(phosphino)amines *erythro*-*i*-PrN[PhP(*i*-PrNH)][PhP(EtNH)] (**4A**), *meso- and d,l-i*-PrN[PhP(*i*-PrNH)]$_2$ (**5A** and **5B**), *erythro-i*-PrN-[PhP(*i*-PrNH)][PhP(*t*-BuNH)] (**6**), *erythro-i*-PrN[PhP(*i*-PrNH)][PhP(PhNH)] (**7**), and *erythro-i*-PrN[PhP-(PhNH)]$_2$ (**8**) have been examined. Compound **8**, newly prepared in this study, and the previously synthesized **4A** and **5A** have been characterized by X-ray single-crystal analysis: **4A**, monoclinic, $P2_1/n$, a = 10.678(4) Å, b = 16.159(12) Å, c = 13.291(4) Å, β = 107.839(26)°, V = 2183(2) Å^3, Z = 4, R = 0.0602, R_w = 0.0898; **5A**, orthorhombic, *Pbca*, a = 10.616(5) Å, b = 16.340(7) Å, c = 26.81(2) Å, V = 4651(4) Å^3, Z = 8, R = 0.0623, R_w = 0.0724; **8**, triclinic, $P\bar{1}$, a = 10.226(5) Å, b = 10.793(4) Å, c = 13.370(6) Å, α = 69.17(3)°, β = 71.13(4)°, γ = 68.86(3)°, V = 1253.8(10) Å^3, Z = 2, R = 0.0602, R_w = 0.0784. Compounds **4A**, **5A**, and **8**, like the previously characterized **6**, all assume a conformation around the P–N–P skeleton in which the assumed lone-pair electron positions are approximately *trans* and parallel to the P_2N molecular plane. ^{31}P NMR spectra of the **4A**, **5A**, **6**, **7**, **8**, and **5A**/**5B** mixtures in solution as a function of temperature show that the bis(phosphino)amines exist as an average of exchanging conformations at 25 °C, but at low temperatures they freeze into preferred conformations. **5A**, **5B**, **6**, and **8** show one conformation at low temperature; **4A** and **7** exist as mixtures of two conformers. Analysis of $^2J_{PNP}$ skeletal P–N–P coupling constants shows that the preferred, lowest energy, conformation is approximately the same as seen in the solid state.

Introduction

Structural properties of bis(phosphino)amines RN(PXX′)$_2$ (**1**) have been studied in order to determine conformational preferences around the P–N–P skeleton[1–20] and the correlation between conformation and $^2J_{PNP}$ coupling constants.[1–4,8–13] Consequently, as a result of NMR spectroscopic, electron, and X-ray diffraction analyses[14,15] and molecular modeling studies,[6] it has been established that the three conformations **1A**, **1B**, and **1C**, of symmetries C_s, C_{2v}, and $C_{2v'}$ (where X = X′), respectively, are most likely. In each conformation, the RN nitrogen is trigonal planar and the phosphorus and RN lone-pair electrons are orthogonal. Isomer **1A** has the phosphorus lone-pair electrons *trans* oriented. Isomers **1B** and **1C** have the lone pairs in *cis* orientations. It has been determined that when the R and X(X′) substituents are relatively small, conformation **1B** is preferred but when the R and/or X(X′) groups are large, as with *i*-PrN-(PPh$_2$)$_2$,[1,2] **1A** is favored. In addition, there is evidence that large positive $^2J_{PNP}$ coupling constants (150–665 Hz) are associated with conformation **1B** whereas small negative $^2J_{PNP}$ values (−15 to −35 Hz) correlate with conformation **1A**. Isomer **1C** appears to be energetically least desirable due to high repulsive interactions between the eclipsed X(X′) groups of the two PX(X′) units and, so far, has not been observed.

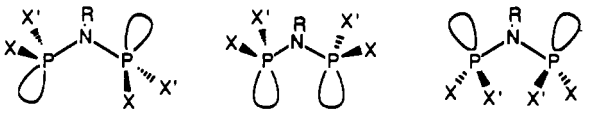

1A (C_s) **1B** (C_{2v}) **1C** ($C_{2v'}$)

Most of the bis(phosphino)amines reported so far have been symmetrically substituted (**1**, X = X′); little is known about unsymmetrically substituted compounds (X ≠ X′), which contain asymmetric phosphorus centers. Interestingly, in condensation reactions between primary amines and the bis(phosphino)amine *erythro*/*threo-i*-PrN[PhP(*i*-PrNH)][PhPCl] (**2A**/**2B**), which form bis(phosphino)amines *i*-PrN[PhP(*i*-PrNH)][PhP(RNH)] (R = Me, **3**; R = Et, **4**; R = *i*-Pr, **5**; R = *t*-Bu, **6**; R = Ph, **7**), the products are formed highly diastereoselectively.[20] Similar diastereoselective reactions could also be important in isomer-specific 1,3,2,4-diazadiphosphetidine formation[21,22] and in the potential stereoregular synthesis of phosphazane (PR–NR′)$_n$ oligomers and polymers.[23]

* Abstract published in *Advance ACS Abstracts,* April 1, 1994.

(1) Keat, R.; Manojlović-Muir, L.; Muir, K. W.; Rycroft, D. S. *J. Chem. Soc., Dalton Trans.* **1981**, 2192 and references cited therein.
(2) Colquhoun, I. J.; McFarlane, W. *J. Chem. Soc., Dalton Trans.* **1977**, 1674.
(3) Cross, R. J.; Green, T. H.; Keat, R. *J. Chem. Soc., Dalton Trans.* **1976**, 1424.
(4) (a) Ebsworth, E. A. V.; Rankin, D. W. H.; Wright, J. G. *J. Chem. Soc., Dalton Trans.* **1977**, 2348. (b) Ebsworth, E. A. V.; Rankin, D. W. H.; Wright, J. G. *J. Chem. Soc., Dalton Trans.* **1979**, 1065.
(5) Harvey, D. A.; Keat, R.; Keith, A. N.; Muir, K. W.; Rycroft, D. S. *Inorg. Chim. Acta* **1979**, *34*, L201.
(6) (a) Keat, R. *Top. Curr. Chem.* **1982**, *102*, 89. (b) Shaw, R. A. *Phosphorus Sulfur* **1978**, *4*, 101.
(7) Chen, H.-J.; Barendt, J. M.; Haltiwanger, R. C.; Hill, T. G.; Norman, A. D. *Phosphorus Sulfur* **1986**, *26*, 155.
(8) Rudolph, R. W.; Newmark, R. A. *J. Am. Chem. Soc.* **1970**, *92*, 1195.
(9) (a) Nixon, J. F. *J. Chem. Soc. A* **1969**, 1087. (b) Nixon, J. F. *J. Chem. Soc. A* **1968**, 2689.
(10) Metzinger, H. G. *Org. Magn. Reson.* **1971**, *3*, 485.
(11) Niecke, E.; Nixon, J. F. *Z. Naturforsch., B* **1972**, *27B*, 467.
(12) Krüger, W.; Schmutzler, R. *Inorg. Chem.* **1979**, *18*, 871.
(13) (a) Hägele, G.; Harris, R. K.; Wazeer, M. I. M.; Keat, R. *J. Chem. Soc, Dalton Trans.* **1986**, 1974. (b) Bulloch, G.; Keat, R.; Rycroft, D. S.; Thompson, D. G. *Org. Magn. Reson.* **1979**, *12*, 708.
(14) Hedberg, E.; Hedberg, L.; Hedberg, K. *J. Am. Chem. Soc.* **1974**, *96*, 4417.
(15) Huntley, C. M.; Laurenson, G. S.; Rankin, D. W. H. *J. Chem. Soc., Dalton Trans.* **1980**, 954.
(16) Barrow, M. J.; Ebsworth, E. A. V.; Harding, M. M.; Henderson, S. G. D. *J. Chem. Soc., Dalton Trans.* **1979**, 1192.
(17) (a) Tarrasoli, A.; Thompson, M. L.; Haltiwanger, R. C.; Hill, T. G.; Norman, A. D. *Inorg. Chem.* **1988**, *27*, 3382. (b) Thompson, M. L.; Tarrasoli, A.; Haltiwanger, R. C.; Norman, A. D. *Inorg. Chem.* **1987**, *26*, 684.
(18) Tarrasoli, A.; Haltiwanger, R. C.; Norman, A. D. *Inorg. Chem.* **1982**, *21*, 2684.
(19) (a) Hill, T. G.; Haltiwanger, R. C.; Prout, T. R.; Norman, A. D. *Inorg. Chem.* **1989**, *28*, 3461. (b) Hill, T. G.; Haltiwanger, R. C.; Norman, A. D. *Inorg. Chem.* **1985**, *24*, 3499.
(20) Prout, T. R.; Imiolczyk, T. W.; Haltiwanger, R. C.; Hill, T. G.; Norman, A. D. *Inorg. Chem.* **1992**, *31*, 215.

0020-1669/94/1333-1783$04.50/0 © 1994 American Chemical Society

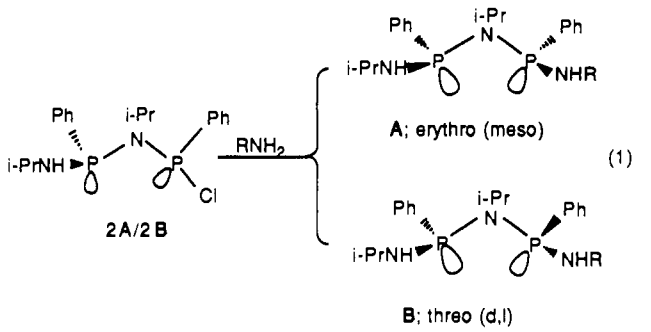

3, R = Me; 4, R = Et; 5, R = i-Pr; 6, R = t-Bu; 7, R = Ph

Of the unsymmetrically substituted bis(phosphino)amines **3A/3B**, **4A/4B**, **5A/5B**, **6**, and **7** prepared earlier,[20] only **6** was unambiguously shown to be the *erythro* isomer. The structure of *meso*-*i*-PrN[PhP(*i*-PrNH)]$_2$ (**5A**) was established, but only indirectly as the molybdenum complex **5A**·Mo(CO)$_4$. Knowing this information and assuming that the same diastereomer is favored in all amine–**2A/2B** reactions, we concluded that in all cases the *erythro* (or *meso* for **5**) isomer is selected. However, it is possible that **5A** was initially the *d,l* diastereomer and that it undergoes a *d,l* to *meso* interconversion during formation of the **5A**·Mo(CO)$_4$ complex. Also, it is not *a priori* necessary that all amine–**2A/2B** reactions proceed with the same stereochemistry. Thus, absolute structure determination for additional, uncomplexed members of the series was needed.

The bis(phosphino)amines **3–7** are also of interest because they constitute the first series of bis(phosphino)amines for which we can obtain both ^{31}P NMR low-temperature spectral and X-ray solid state data. It becomes possible to compare structural features of the compounds in solution with those in the solid state and to determine if the lowest energy conformations in solution correlate with those seen in the solid. Finally, the possibility exists that differences might be observed in conformational behavior between *erythro* (or *meso*) and *threo* (or *d,l*) isomers. Thus, in order to better understand the structural and conformational properties of bis(phosphino)amines, we now report (i) studies of the variable-temperature ^{31}P NMR spectra of the *erythro* (or *meso*) diastereomers **4A**, **5A**, **6**, and **7**, the new *erythro*-*i*-PrN[Ph(PhNH)]$_2$ (**8**), and the *meso*/*d,l* mixture **5A/5B** and (ii) the X-ray structural data for the compounds **4A**, **5A**, and **8**, making available complete structural data for the series of related compounds **4A**, **5A**, **6**,[20] and **8**.

Experimental Section

Apparatus and Materials. All operations were carried out in N_2-flushed glovebags and standard vacuum-line equipment.[24] Infrared and mass spectra were obtained using IBM FTIR (IR/32 Type 9132) and VG Analytical 7070 EQ-HF spectrometers. Elemental analyses were performed by Huffman Labs, Golden, CO. X-ray crystallographic data were collected at room temperature using a Nicolet Analytical Instruments P3/F automated diffractometer (Mo Kα radiation, graphite monochromator). ^{1}H (300 MHz) NMR spectra were recorded on a Varian Associates VXR 300S spectrometer, and ^{31}P NMR spectra were obtained on JEOL FX-90Q (36.3 MHz) and Bruker WM-250 (101.2 MHz), VXR 300S (121.4 MHz), and VXR 500S (202.4 MHz) spectrometers. ^{1}H and ^{31}P NMR chemical shifts (+δ = downfield) were measured relative to internal Me_4Si and external 85% H_3PO_4, respectively. In cases where ^{31}P NMR relative spectral areas were important (e.g. **5A:5B**, below), the areas measured in decoupled [^{31}P{^{1}H}] spectra were compared to those in undecoupled [^{31}P] spectra and the instrumentation data collection conditions were varied over a wide range. In all cases, area agreement was within ±10%. Variable-temperature experiments were carried out in toluene/benzene-d_6 (10%) or toluene-d_8 unless otherwise stated. Temperature calibrations were accomplished using a Fluke thermocouple gauge (JEOL FX90Q) and a standard methanol sample with a calibration error of ±1.0 °C (Varian VXR 300S). Calculated spectra for the *i*-PrN[PhP(*i*-PrNH)]$_2$ (**5A**) series were produced with the program DNMR-4[25] on a MicroVAX II computer. In order to plot the simulated spectra, the ADPLOT[25] program was rewritten for compatibility with the GKS drawing package on the MicroVAX II.

All solvents were freshly distilled and stored under N_2. *erythro*/*threo*-*i*-PrN[PhP(*i*-PrNH)][PhPCl] (**2A/2B**), *i*-PrN[PhP(*i*-PrNH)][PhP(*t*-BuNH)] (**6**), and *i*-PrN[PhP(*i*-PrNH)][PhP(PhNH)] (**7**) were obtained as described previously.[20] *meso*-*i*-PrN[PhP(*i*-PrNH)]$_2$ (**5A**) and *erythro*-*i*-PrN[PhP(*i*-PrNH)][PhP(EtNH)] (**4A**) were obtained by fractional crystallization from *meso*/*d,l*-*i*-PrN[PhP(*i*-PrNH)]$_2$ (**5A/5B**) and *erythro*/*threo*-*i*-PrN[PhP(*i*-PrNH)][PhP(EtNH)] (**4A/4B**) mixtures as reported earlier.[19,20] $PhPCl_2$ (Strem Chemicals) was distilled before use. Et_3N (Baker Chemical), *i*-$PrNH_2$ (Aldrich), and $PhNH_2$ (Aldrich) were distilled from CaH_2. Toluene (Fisher Scientific) was distilled from Na/Pb alloy. CD_2Cl_2, benzene-d_6, and toluene-d_8 (Aldrich) were used as obtained.

From a **4A/4B** or **5A/5B** mixture it was possible to isolate as crystalline products only the major isomer, **4A** or **5A**. Neither **3A** nor **3B** could be obtained pure. ^{31}P NMR data for **5B** were obtained on **5A/5B** mixtures and are reported as such. **5A/5B** mixtures, enriched to **5A:5B** = 1:1, were obtained by repeated crystallizations from solutions which had initial **5A:5B** ratios of (10–12):1. Spectra of **5A/5B** mixtures versus temperature were carried out at 300 and 500 MHz to allow assignment of overlapped resonances.

***i*-PrN[PhP(PhNH)]$_2$ (8).** Aniline (3.95 g, 42.4 mmol) in toluene (10 mL) was added to a solution of **2A/2B** (16.2 mmol) in toluene (25 mL). After 24 h at room temperature, $PhNH_3Cl$ was removed by filtration. ^{31}P NMR spectral analysis showed singlets at δ 57.0 and 45.3 for **8** and $PhP(PhNH)_2$,[18] respectively (mole ratio 1.1:1). Recrystallization from toluene yielded **8** (mp 144–146 °C; yield 60–70%). Anal. Calcd for $C_{27}H_{29}P_2N_3$: C, 70.95; H, 6.41; N, 9.19; P, 13.55. Found: C, 69.74; H, 6.58; N, 9.46; P, 13.42. MS (EI$^+$): $(M+1)^+$ *m*/*e* (% rel int) 457 (10.4) [$C_{27}H_{29}P_2N_3^+$]. MS (CI): M^+ *m*/*e* (% rel int) 456 (100) [$C_{27}H_{28}P_2N_3^+$]. IR (KBr, cm^{-1}): 3331 (w), 3057 (m), 1237 (vs), 1176 (vs), 997 (vs), 700 (m). ^{31}P{^{1}H} NMR (36.4 MHz, toluene): δ 56.9 (s). ^{1}H NMR (CD_2Cl_2): δ 1.28 [d, $^2J_{HH}$ = 6.59 Hz, area 6; $CH(CH_3)_2$], 3.35 [m, area 1; $CH(CH_3)_2$], 5.01 (d of d, area 2; NH), 6.75–7.47 (m, area 20; C_6H_5).

In a separate experiment, $PhNH_2$ (1.45 g, 15.6 mmol) in toluene (10 mL) was added to a solution of **2A/2B** (7.8 mmol) in toluene (25 mL) and the mixture was stirred for 72 h at room temperature. ^{31}P NMR spectral analysis showed two doublets at δ 63.0 and 54.6 for *i*-PrN[PhP(*i*-PrNH)][PhP(PhNH)] (**7**) as well as two singlets at δ 56.9 and 45.3 for **8** and $PhP(PhNH)_2$,[18] respectively (mole ratio 40:8:2). Additional $PhNH_2$ (8.7 mmol) was introduced, and the solution was heated at 74–82 °C for 120 h. ^{31}P NMR spectral analysis of this sample showed mainly two singlets due to **8** and $PhP(PhNH)_2$ (ratio 1:2).

Reactions of $PhNH_3Cl$. (A) With *meso*-*i*-PrN[PhP(*i*-PrNH)]$_2$ (5A). A $PhNH_3Cl$-saturated toluene solution which contained excess solid $PhNH_3Cl$ was added to **5A** in toluene, and the mixture was heated at 80 °C. After 4 h, ^{31}P NMR analysis of the solution showed **2A/2B** (δ 126.1, 65.7, 62.0),[20] **5A**, and $PhP(NHPh)_2$.

(B) With *i*-PrN[PhP(*i*-PrNH)][PhP(PhNH)] (7). Excess $PhNH_3Cl$ was added to **7** in toluene. After 2.5 h at 25 °C and 1.5 h at 80 °C, the ^{31}P NMR spectrum showed signals for **2A/2B** and $PhP(NHPh)_2$ and an unassigned singlet at δ 54.5.

Variable-Temperature ^{31}P NMR Spectral Analysis. ^{31}P NMR spectra of **4A**, **5A**, **6**, **7**, **8**, and **5A/5B** in toluene-d_8 were obtained in the range +25 to −95 °C studies of. Temperatures were measured to ±1 °C. Spectra of **5A** were simulated using the program DNMR-4, and spectra were plotted using a modified version of the program ADPLOT.[25] The pseudo-first-order rate constants (k) for exchange were obtained by fitting the calculated to the experimental spectra. Only the **5A** spectral series was simulated, since the rate constant values at T_c were the same (within experimental error) as those obtained using the rate constant approxima-

(21) Chen, H.-J.; Haltiwanger, R. C.; Hill, T. G.; Thompson, M. L.; Coons, D. E.; Norman, A. D. *Inorg. Chem.* **1985**, *24*, 4725.
(22) Bulloch, G.; Keat, R.; Thompson, D. G. *J. Chem. Soc., Dalton Trans.* **1977**, 99.
(23) Bent, E. G.; Barendt, J. M.; Haltiwanger, R. C.; Norman, A. D. *Inorganic and Organometallic Polymers*; ACS Symposium, Series 360; American Chemical Society: Washington, DC, 1988; p 303.
(24) Shriver, D. F.; Drezdzon, M. A. *The Manipulation of Air-Sensitive Compounds*, 2nd ed; Wiley-Interscience: New York, 1986.
(25) Bushweller, H. C.; Letendre, L. J.; Brunelle, J. A.; Bilofsky, H. S.; Whalon, M. R.; Fleischman, S. H. *QCPE* **1978**, Program 466. See also: Binsch, G. *J. Magn. Reson.* **1978**, *30*, 625. DNMR-4 is a modification of DNMR-3: Kleier, D. A.; Binsch, G. *QCPE* **1969**, Progam 165.

Table 1. Crystallographic Data for *erythro-i*-PrN[PhP(*i*-PrNH)][PhP(EtNH)] (**4A**), *meso-i*-PrN[PhP(*i*-PrNH)]$_2$ (**5A**), and *meso-i*-PrN[PhP(PhNH)]$_2$ (**8**)

	4A	**5A**	**8**
formula	$C_{20}H_{31}N_3P_2$	$C_{21}H_{33}N_3P_2$	$C_{27}H_{29}N_3P_2$
fw	375.43	389.4	457.5
space group	$P2_1/n$	*Pbca*	$P\bar{1}$
a, Å[a]	10.678(4)	10.616(5)	10.226(5)
b, Å	16.159(12)	16.340(7)	10.793(4)
c, Å	13.291(4)	26.81(2)	13.370(6)
α, deg	90.0	90.0	69.17(3)
β, deg	107.84(3)	90.0	71.13(4)
γ, deg	90.0	90.0	68.86(3)
V, Å^3	2183(2)	4651(4)	1253.8(10)
d_{calcd}, g/cm^3	1.14	1.112	1.212
Z	4	8	2
μ, cm^{-1}	2.0	1.91	1.87
λ(Mo Kα), Å	0.710 73	0.710 73	0.710 73
T, °C	22–24	22–24	22–24
R[b]	0.0602	0.0623	0.0602
R_w	0.0898	0.0724	0.0784

[a] Estimated standard deviations in the least significant figure(s) are given in parentheses in this and all subsequent tables. [b] Based on observed data.

tions $k_c = \pi(\Delta\nu)/2^{1/2}$ and $k_c = \pi\{0.5[(\Delta\nu)^2 + 6(^2J_{AB})^2]\}^{1/2}$, where $\Delta\nu$ and $^2J_{AB}$ are the chemical shift separations between the resonances ν_A and ν_B in hertz and their coupling constant values, respectively, measured in the region of slow exchange.[26] The values for the free energy of activation (ΔG^*) for the dynamic process were derived from the Eyring equation $k_c = [\kappa(k_bT_c)/h]\exp(-\Delta G^*/RT_c)$, where k_b is the Boltzmann constant, T_c is the temperature at coalescence, h is Planck's constant and R is the ideal gas constant. A transmission coefficient (κ) of unity is assumed. Rearrangement of this equation yields $\Delta G^* = RT_c(23.76 + (\ln T_c)/k)$ (in kJ/mol), from which ΔG^* values were calculated using the above approximations for k and T_c values from the measured spectra. The ΔG^* values are taken to be accurate within ±1 kJ/mol.[27]

X-ray Structure Analyses. (A) ***erythro-i*-PrN[PhP(*i*-PrNH)][PhP(EtNH)] (4A).** An X-ray-quality crystal, obtained from toluene, was mounted on a glass fiber and coated with epoxy resin. Crystal data and details of the data collection and structure refinement are summarized in Table 1. Cell parameters were determined on the diffractometer and refined by a least-squares fit to 25 centered reflections in the range 26.8° ≤ 2θ ≤ 34.5°. The structure was solved by direct methods.[28] The molecule was refined anistropically, except for the hydrogen atoms, which were included in idealized positions. Amine hydrogens refined into positions corresponding to sp^2 hybridization and therefore were included in idealized positions. Final positional parameters for **4A** are given in Table 2. Thermal parameters and full metrical details are included in the supplementary material.

(B) ***meso-i*-PrN[PhP(*i*-PrNH)]$_2$ (5A).** An X-ray-quality crystal, obtained from decane, was mounted on a glass fiber. Crystal data and details of the data collection and structure refinement are summarized in Table 1. Cell parameters were determined on the diffractometer and refined by a least-squares fit to 25 centered reflections in the range 24.3° ≤ 2θ ≤ 33.8°. The structure was solved by direct methods.[28] The molecule was refined anistropically, except for the hydrogen atoms. Hydrogen atoms were included in idealized positions and, with the exception of the amine hydrogens, were refined riding on the atom to which they were attached with one overall isotropic displacement parameter for the entire set of hydrogens. The amine hydrogens were refined with no positional constraints and with individual isotropic displacement parameters. Final positional parameters for **5A** are given in Table 3. Thermal parameters and full metrical details are included in the supplementary material.

(C) ***meso-i*-PrN[PhP(PhNH)]$_2$ (8).** An X-ray-quality crystal, obtained from decane, was mounted on a glass fiber. Crystal data and details of the data collection and structure refinement are summarized in Table 1. Cell parameters were determined on the diffractometer and refined by a least-squares fit to 25 centered reflections in the range 29.6° ≤ 2θ ≤ 35.7°. The structure was solved by direct methods. The molecule was refined anistropically, except for the hydrogen atoms.[28] Hydrogen atoms were included in idealized positions and, with the exception of the amine hydrogens, were refined riding on the atom to which they were attached with isotropic displacement parameters for the hydrogens refined as overall parameters for the various types of hydrogens, i.e. one isotropic displacement parameter for the methyl group hydrogens and others for each of the phenyl groups. The amine hydrogens were refined with no positional constraints and with individual isotropic displacement parameters. Final positional parameters for **8** are given in Table 4.

Table 2. Atomic Coordinates (×10^4) and Equivalent Isotropic Displacement Parameters (Å^2 × 10^3) for *erythro-i*-PrN[PhP(EtNH)][PhP(*i*-PrNH)] (**4A**)

	x	y	z	U_{eq}[a]
P(1)	–64(1)	2957(1)	45(1)	69(1)
P(2)	1870(1)	3668(1)	1941(1)	64(1)
N(1)	–1109(3)	3721(3)	118(3)	83(2)
N(2)	1049(3)	2829(2)	1277(2)	64(1)
N(3)	3429(3)	3390(2)	2522(3)	76(1)
C(17)	–2421(5)	3578(5)	152(6)	125(3)
C(27)	1230(5)	1985(3)	1760(4)	84(2)
C(37)	4484(5)	3629(4)	2145(4)	93(2)
C(18)	–3322(6)	4224(5)	–334(6)	146(4)
C(29)	2104(6)	1450(3)	1322(5)	119(3)
C(28)	–28(6)	1540(4)	1673(5)	123(3)
C(39)	5553(7)	4056(5)	2960(7)	163(4)
C(38)	5214(9)	2969(6)	1909(7)	200(6)
C(11)	888(4)	3503(3)	–666(3)	63(2)
C(12)	327(5)	4104(3)	–1419(3)	78(2)
C(13)	1015(6)	4413(3)	–2065(4)	94(2)
C(14)	2250(6)	4142(4)	–1970(4)	97(3)
C(15)	2825(5)	3563(3)	–1238(4)	89(2)
C(16)	2158(4)	3244(3)	–595(3)	76(2)
C(21)	1312(4)	3692(2)	3116(3)	64(2)
C(22)	2079(5)	4056(3)	4045(3)	88(2)
C(23)	1593(6)	4159(4)	4889(4)	111(3)
C(24)	368(7)	3906(4)	4836(4)	103(3)
C(25)	–406(5)	3572(3)	3937(4)	95(2)
C(26)	50(5)	3456(3)	3078(4)	82(2)

[a] Equivalent isotropic U defined as one-third of the trace of the orthogonalized U_{ij} tensor.

Table 3. Atomic Coordinates (×10^4) and Equivalent Isotropic Displacement Parameters (Å^2 × 10^3) for *meso-i*-PrN[PhP(*i*-PrNH)]$_2$ (**5A**)

	x	y	z	U_{eq}[a]
P(1)	–5342(2)	9430(1)	1209(1)	48(1)
P(2)	–4211(2)	7822(1)	1481(1)	54(1)
N(1)	–4670(6)	10146(4)	857(3)	65(3)
N(2)	–4760(5)	8496(3)	1037(2)	49(2)
N(3)	–5405(7)	7606(4)	1852(3)	72(3)
C(27)	–4728(7)	8234(4)	505(2)	59(3)
C(28)	–5338(8)	7408(5)	420(3)	79(3)
C(29)	–3387(7)	8241(5)	310(3)	79(3)
C(11)	–6916(6)	9402(4)	929(2)	49(2)
C(12)	–7652(7)	8714(5)	993(2)	63(3)
C(13)	–8908(7)	8698(5)	845(3)	75(3)
C(14)	–9441(8)	9363(7)	635(3)	86(4)
C(15)	–8754(9)	10057(6)	574(3)	87(4)
C(16)	–7491(8)	10080(5)	720(2)	69(3)
C(17)	–3738(8)	10724(4)	1040(3)	71(3)
C(18)	–2597(8)	10760(5)	725(4)	120(5)
C(19)	–4312(9)	11560(5)	1080(4)	112(4)
C(21)	–3247(6)	8532(4)	1853(3)	54(3)
C(22)	–3437(7)	8683(5)	2355(3)	70(3)
C(23)	–2644(10)	9180(6)	2618(3)	86(4)
C(24)	–1627(10)	9518(6)	2397(4)	93(4)
C(25)	–1389(8)	9351(6)	1907(4)	93(4)
C(26)	–2201(7)	8882(5)	1635(3)	76(3)
C(37)	–5859(9)	6788(6)	1943(4)	93(4)
C(38)	–5818(13)	6586(7)	2491(5)	207(8)
C(39)	–7128(12)	6663(7)	1809(5)	187(8)

[a] Equivalent isotropic U defined as one-third of the trace of the orthogonalized U_{ij} tensor.

(26) (a) Sandstrom, J. *Dynamic NMR Spectroscopy*; Academic Press: London, 1982. (b) Kost, D.; Carlsen, E. H.; Raban, M. *Chem. Commun.* **1971**, 656.
(27) Kessler, H. *Angew. Chem., Int. Ed. Engl.* **1970**, *9*, 219.
(28) Sheldrick, G. M. *SHELXTL-PLUS: A Program for Crystal Structure Determination*, Version 3.4; Nicolet Analytical Instruments: Madison, WI, 1988; performed on a Micro VAX II.

Table 4. Atomic Coordinates ($\times 10^4$) and Equivalent Isotropic Displacement Parameters ($Å^2 \times 10^3$) for *meso*-*i*-PrN[PhP(PhNH)]$_2$ (**8**)

	x	*y*	*z*	U_{eq}[a]
P(1)	4690(1)	8138(1)	8425(1)	52(1)
P(2)	3393(1)	9081(1)	6485(1)	54(1)
N(1)	6135(3)	8616(4)	7516(3)	61(2)
N(3)	1630(3)	9342(4)	6555(3)	63(2)
N(2)	3778(3)	7877(3)	7677(2)	52(1)
C(27)	3425(4)	6535(4)	8064(3)	60(2)
C(28)	4745(5)	5285(4)	8245(5)	93(3)
C(29)	2208(5)	6479(5)	9077(4)	84(2)
C(11)	3628(4)	9815(4)	8672(3)	52(2)
C(12)	4279(5)	10635(4)	8824(4)	76(2)
C(13)	3468(6)	11791(5)	9197(4)	90(3)
C(14)	1988(6)	12152(5)	9402(4)	86(3)
C(15)	1335(5)	11358(5)	9265(4)	86(3)
C(16)	2133(4)	10183(5)	8912(4)	72(2)
C(21)	4177(4)	8020(4)	5513(3)	57(2)
C(22)	3491(5)	8031(5)	4772(3)	73(2)
C(23)	4180(7)	7263(6)	4015(4)	96(3)
C(24)	5586(6)	6490(6)	3992(5)	103(3)
C(25)	6299(6)	6468(6)	4699(4)	90(3)
C(26)	5612(4)	7229(5)	5451(4)	74(2)
C(31)	7546(3)	7733(4)	7355(3)	53(2)
C(32)	8490(4)	7991(5)	6347(4)	69(2)
C(33)	9893(5)	7127(6)	6210(5)	86(3)
C(34)	10341(5)	6036(6)	7050(5)	92(3)
C(35)	9396(5)	5769(5)	8038(5)	89(3)
C(36)	7995(4)	6621(5)	8203(4)	70(2)
C(41)	527(4)	10425(4)	6936(3)	60(2)
C(42)	696(6)	11727(5)	6589(4)	81(2)
C(43)	−385(7)	12797(6)	6976(5)	103(3)
C(44)	−1608(7)	12545(8)	7705(6)	118(4)
C(45)	−1788(5)	11252(8)	8051(5)	109(4)
C(46)	−738(4)	10183(5)	7670(4)	78(2)

[a] Equivalent isotropic U defined as one-third of the trace of the orthogonalized U_{ij} tensor.

Thermal parameters and full metrical details are included in the supplementary material.

Results and Discussion

Several of the bis(phosphino)amines studied in this work, **4A**, **5A**, **5B**, **6** and **7**, had been prepared previously; however, only *erythro*-*i*-PrN[PhP(*i*-PrNH)][PhP(*t*-BuNH)] (**6**) and **5A**, as the **5A**·Mo(CO)$_4$ complex, had been characterized by X-ray analysis.[18] Now, we have obtained X-ray structures for **4A**, uncomplexed **5A**, and the newly prepared single diastereomer of *i*-PrN[PhP(PhNH)]$_2$ (**8**). From our previous studies and those conducted herein, we can conclude that the major, and in some cases exclusive, product of reactions of **2A/2B** mixtures with primary amines is the *erythro* (*meso*) diastereomer.

The bis(phosphino)amine **8** forms from reaction of **2A/2B** with excess $PhNH_2$ (**2**:$PhNH_2$ = 2.5:1, m/m) according to eq 2. The

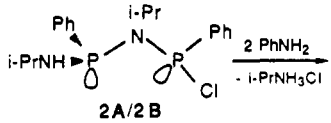

2A/2B

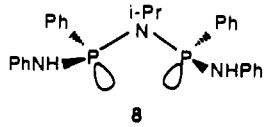

8 (2)

reaction apparently proceeds through formation of *i*-PrN[PhP(*i*-PrNH)][PhP(PhNH)] (**7**). In a **2A/2B** reaction with less than 2.5 equiv of $PhNH_2$, **7** is shown by ^{31}P NMR spectral analysis to be a major reaction product (eq 3a, Scheme 1). When additional $PhNH_2$ is added to this solution and the reaction is allowed to proceed further, the system yields mainly **8**. Some

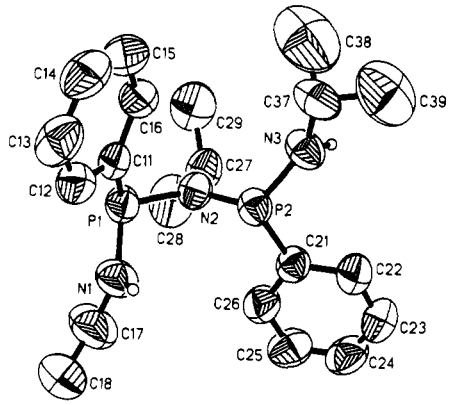

Figure 1. Structure and numbering scheme for *erythro*-*i*-PrN[PhP(*i*-PrNH)][PhP(EtNH)] (**4A**). Thermal ellipsoids are shown at the 50% probability level. Hydrogen atoms are omitted for clarity.

Scheme 1

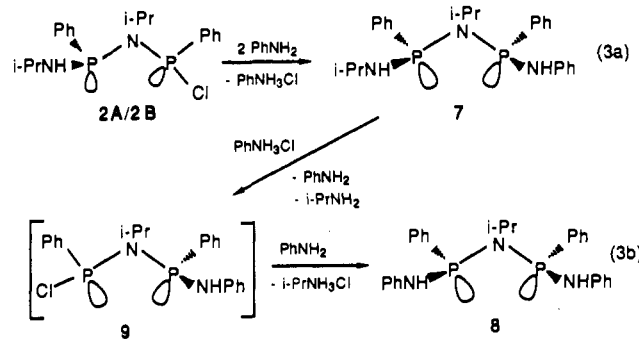

formation of $PhP(NHPh)_2$ occurs in these reactions; this may be the result of competing diphosphazane skeletal cleavage reaction(s) which is (are) unrelated to the formation of **8**. How **7** is converted to **8** is unclear; however, it seems unlikely that it occurs via $PhNH_2$ transamination of **7** since in other studies we have established that transaminations require much more vigorus reaction conditions.[20] Possibly, $PhNH_3Cl$ catalyzes this reaction by forming the chloro amino intermediate **9**, which could result from cleavage of the *i*-PrNH group from **7**. We have not observed **9**, but since we know that $PhNH_3Cl$ cleaves **5A** to form **2A/2B**, a similar process to yield **9** is possible. The $PhNH_3Cl$ could cleave either an *i*-PrNH– or a PhNH– group from **7** to give **2A/2B** or **9**, respectively; however subsequent reaction of $PhNH_2$ with **2A/2B** would only regenerate **7**, whereas $PhNH_2$ reaction with **9** would lead to **8** (eq 3b). The overall reaction should be driven to **8** because (i) *i*-$PrNH_2$ is more basic than $PhNH_2$,[29] a situation which favors the system's formation of *i*-$PrNH_3Cl$, and (ii) *i*-$PrNH_3Cl$ is less soluble than $PhNH_3Cl$ in toluene, causing precipitation of *i*-$PrNH_3Cl$.

The structures of **4A**, **5A**, and **8**, determined by X-ray single-crystal analysis, are shown in Figures 1–3, respectively. In every case, the compound is the *erythro* (*meso* for **5A**), diastereomer and has a conformation where the P–N–P skeletal conformation is approximately of the *trans* **1A** type. The electron pair on one phosphorus is *cis* to the central *i*-Pr group; the other phosphorus electron pair is *trans*. Selected bond distances and angles for **4A**, **5A**, and **8** are given in Tables 5–7, and a comparison of selected structural parameters, including skeletal conformational twist angles for the 4A, 5A, the previously studied 6,[20] and 8 series, is shown in Table 8 Interestingly, the distances and angles are very similar within the series and similar to those of other known bis(phosphino)amines. In every case the P(1)/N(2)/P(2)/C(27) skeleton is planar; the sums of the angles around N(2) are 359.9,

(29) March, J. *Advanced Organic Chemistry*, 3rd ed.; Wiley-Interscience: New York, 1985.

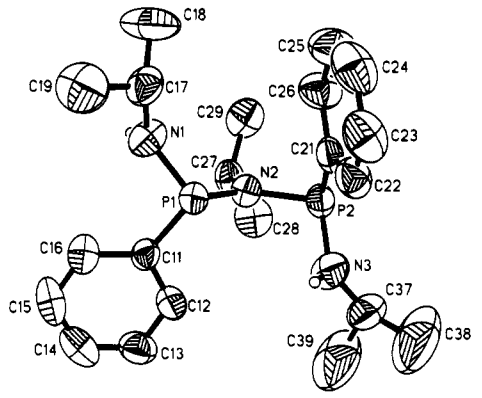

Figure 2. Structure and numbering scheme for *meso-i*-PrN[PhP(*i*-PrNH)]$_2$ (**5A**). Thermal ellipsoids are shown at the 50% probability level. Hydrogen atoms are omitted for clarity.

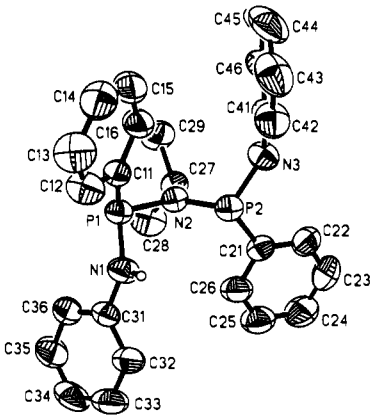

Figure 3. Structure and numbering scheme for *erythro-i*-PrN[PhP(PhNH)]$_2$ (**8**). Thermal ellipsoids are shown at the 50% probability level. Hydrogen atoms are omitted for clarity.

Table 5. Selected Structural Parameters for *erythro-i*-PrN[PhP(EtNH)][PhP(*i*-PrNH)] (**4A**)

	(a) Bond Distances (Å)		
P(1)–N(1)	1.687(4)	P(1)–N(2)	1.716(3)
P(1)–C(11)	1.815(5)	P(2)–N(2)	1.705(3)
P(2)–N(3)	1.668(3)	P(2)–C(21)	1.833(5)
N(1)–C(17)	1.434(7)	N(2)–C(27)	1.495(6)
N(3)–C(37)	1.420(7)		
	(b) Bond Angles (deg)		
N(1)–P(1)–N(2)	108.1(2)	N(1)–P(1)–C(11)	99.2(2)
N(2)–P(1)–C(11)	102.8(2)	N(2)–P(2)–N(3)	107.9(2)
N(2)–P(2)–C(21)	102.0(2)	N(3)–P(2)–C(21)	98.6(2)
P(1)–N(1)–C(17)	123.6(4)	P(1)–N(2)–P(2)	119.6(2)
P(1)–N(2)–C(27)	118.7(3)	P(2)–N(2)–C(27)	121.6(2)
P(2)–N(3)–C(37)	123.4(3)		

359.0, and 359.9° for **4A**, **5A**, and **8**, respectively. As was the case for **6**,[20] and other bis(phosphino)amines such as *i*-PrN(PPh)$_2$[1] and PhN[P(PhNH)$_2$]$_2$,[6,18] the skeletal P–N bonds are somewhat longer [1.705–1.722 Å; mean 1.714(4) Å] than the *exo* P–N bonds [1.650–1.694 Å; mean, 1.677(4) Å].

The conformational orientations of the PhP(NHR)– groups with respect to each other and the P–N–P skeletal plane in **4A**, **5A**, **6**, and **8** are closely similar (Table 8). In each case, the phosphorus lone pairs are essentially *trans* as in conformation **1A**. Conformations can be expressed in terms of two dihedral angles θ_1 and θ_2 (Figure 4), which are dihedral angles between the central P/N/P plane [P(1)/N(2)/P(2)] and the P–L (L = lone pair) vectors that are taken to be perpendicular to the N(1)/N(2)/C(11) and N(3)/N(2)/C(21) planes. These vectors approximate the phosphorus lone-pair electron positions; θ angles are defined as positive (+) and negative (–) when measured above and below the P_2N plane, respectively. The small differences

Table 6. Selected Structural Parameters for *meso-i*-PrN[PhP(*i*-PrNH)]$_2$ (**5A**)

	(a) Bond Distances (Å)		
P(1)–N(1)	1.663(7)	P(1)–N(2)	1.710(5)
P(1)–C(11)	1.832(7)	P(2)–N(2)	1.722(5)
P(2)–N(3)	1.650(7)	P(2)–C(21)	1.841(7)
N(1)–C(17)	1.453(10)	N(2)–C(27)	1.488(8)
N(3)–C(37)	1.442(11)		
	(b) Bond Angles (deg)		
N(1)–P(1)–N(2)	108.7(3)	N(1)–P(1)–C(11)	100.2(3)
N(2)–P(1)–C(11)	101.4(3)	N(2)–P(2)–N(3)	107.1(3)
N(2)–P(2)–C(21)	99.3(3)	N(3)–P(2)–C(21)	103.6(3)
P(1)–N(1)–C(17)	123.9(6)	P(1)–N(2)–P(2)	120.4(3)
P(1)–N(2)–C(27)	121.5(4)	P(2)–N(2)–C(27)	118.1(4)
P(2)–N(3)–C(37)	123.9(6)		

Table 7. Selected Structural Parameters for *meso-i*-PrN[PhP(PhNH)]$_2$ (**8**)

	(a) Bond Distances (Å)		
P(1)–N(1)	1.694(4)	P(1)–N(2)	1.715(4)
P(1)–C(11)	1.828(4)	P(2)–N(3)	1.697(4)
P(2)–N(2)	1.717(3)	P(2)–C(21)	1.834(5)
N(1)–C(13)	1.411(4)	N(3)–C(41)	1.414(5)
N(2)–C(27)	1.490(5)		
	(b) Bond Angles (deg)		
N(1)–P(1)–N(2)	106.1(2)	N(1)–P(1)–C(11)	98.3(2)
N(2)–P(1)–C(11)	103.8(2)	N(3)–P(2)–N(2)	106.8(2)
N(3)–P(2)–C(21)	98.3(2)	N(2)–P(2)–C(21)	101.1(2)
P(1)–N(1)–C(31)	124.8(3)	P(2)–N(2)–C(27)	121.8(3)
P(1)–N(2)–P(2)	120.7(2)	P(1)–N(2)–C(27)	117.4(3)
P(2)–N(3)–C(41)	122.6(4)		

Table 8. Selected Structural Parameters for Bis(phosphino)amines

cmpd	internal P–N (mean), Å	P–N–P deg	θ_1,[a] deg	θ_2,[a] deg	Θ, deg
4A	1.711(3)	119.6(2)	178	–6	172
5A	1.716(5)	120.4(3)	–1	–169	168
6[b]	1.715(3)	120.4(2)	170	–1	171
8	1.716(4)	120.7(2)	–179	0	179
i-PrN(PPh$_2$)$_2$[c]	1.709(4)	122.8	n/a	n/a	n/a

[a] θ_1 and θ_2 are dihedral angles between planes P(1)/P(2)/N(2) and perpendiculars to planes N(2)/N(1)/C(11) and N(2)/N(3)/C(21), respectively. Rotations above and below are defined as + and –, respectively. [b] Data from ref 20. [c] From data in ref 1.

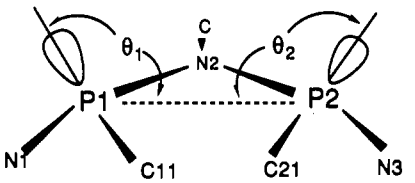

Figure 4. Angles θ_1 and θ_2 in bis(phosphino)amines. Angles measured above and below the central P_2N plane are given as positive (+) and negative (–), respectively.

observed in θ_1, θ_2, or Θ indicate that the conformations are not greatly affected by the PhP(RNH) R-group sizes. The small differences observed may be the result of packing forces in the solid.

Information about the conformational states of the bis(phosphino)amines **4A**, **5A**, **6**, **7**, and **8** as a function of temperature was obtained from ^{31}P NMR spectra obtained at low temperatures.[30-31] In addition, limited comparisons between *meso* and *d,l* diastereomers were made by examination of **5A**/**5B** mixtures. Data from the ^{31}P NMR VT experiments are summarized in Table 9. The compounds exhibit similar spectra

(30) (a) Cowley, A. H.; Taylor, M. W.; Whangbo, M.-H.; Wolfe, S. *J. Chem. Soc., Chem. Commun.* **1976**, 838. (b) Cowley, A. H.; Dewar, M. J. S.; Jackson, W. R. *J. Am. Chem. Soc.* **1968**, *90*, 4185.
(31) Burdon, J.; Hotchkiss, J. C.; Jennings, W. B. *J. Chem. Soc., Perkin Trans. 2* **1976**, 1052.

Table 9. $^{31}P\{^1H\}$ NMR VT Data for the *i*-PrN[PhP(NHR)][PhP(NHR')] Series

			δ ($^2J_{PNP}$, Hz[a])			
cmpd	R	R'	27 °C	−90 °C	T_c,[b] °C	ΔG^*, kJ/mol
4A	*i*-Pr	Et	60.9, 64.8 (13.4)	69.3, 55.4 (15.9) (**4Aa**) 67.0, 60.0 (17.9) (**4Ab**)	−46	44
5A	*i*-Pr	*i*-Pr	60.1	66.2, 56.2 (15.9)	−36[d]	41
5B	*i*-Pr	*i*-Pr	59.1	65.6, 53.2 (12.8)[c]	−40	42
6	*i*-Pr	*t*-Bu	62.4, 49.3 (14.6)	67.6, 46.8 (15.9)	−50	43
7	*i*-Pr	Ph	62.8, 54.7 (12.2)	68.0, 50.0 (12.2) (**7a**) 60.2, 58.5 (20.8) (**7b**)	−45	43
8	Ph	Ph	56.9	61.0, 51.1 (15.9)	−43	43

[a] Absolute values; signs not determined. [b] Estimated from spectral data unless specified otherwise. [c] Spectra measured at 121.4 MHz for a mixture of diastereomers; **5A**:**5B** = 1:1.2. [d] Obtained by curve fitting of simulated spectra; see ref 26.

as a function of temperature; in each case, spectra broaden, coalesce, and then develop into well-defined AX or AB patterns at low temperatures. By comparison of ^{31}P NMR chemical shift (δ) data for **4A**, **6**, and **7** with each other and with those for **5A**, we can assign the low-field and high-field resonances of **4A**, **6**, and **7** to the PhP(*i*-PrNH)– and PhP(RNH)– (R = Et, Ph, *t*-Bu) ends of the molecules, respectively. The low-temperature conformations all show small $^2J_{PNP}$ coupling constants (12–21 Hz). The observed temperature dependence is assumed to result from restricted rotation around skeletal P–N bonds, which results in conformational "freezing" at low temperatures. In every case, the ambient-temperature spectra appeared to be the result of averaged conformations but at reduced temperatures the molecules adopted a distinct frozen conformation or conformations which we take to be the lowest energy conformations for the particular system.

Compounds **5A**, **6**, and **8** freeze to a single conformation, within the limits of our detection ability, below −60 °C. The $^{31}P\{^1H\}$ NMR spectra of **5A** as a function of temperature, which constitute a typical series, are shown in Figure 5. **5A** and **8** both exhibit a singlet resonance at 20 °C, consistent with that expected for a conformationally averaged symmetrical bis(phosphino)amine. At ca. −20 °C, spectral broadening is evident, and by −60 °C, two distinct resonances appear. By −95 °C, the individual resonances of a "frozen"[11] unsymmetrical conformer are well resolved. The frozen-conformer $^2J_{PNP}$ coupling constants of **5A** and **8** are 15.9 and 15.9 Hz, respectively. Compound **6**, because it is an unsymmetrically substituted bis(phosphino)amine, shows two resonances at 27 °C. These broaden below −30 °C and, by −75 °C, split into two coupled ($^2J_{PNP}$ = 15.9 Hz) equal-area resonances. The $^2J_{PNP}$ coupling constants for the frozen conformers of **5A**, **6**, and **8** are small and essentially equal, suggesting that the lowest energy conformations of these three compounds are structurally closely similar.

The VT $^{31}P\{^1H\}$ NMR spectra of **4A** and **7** are more complex, as they show detectable populations of two conformers (**a** and **b**) at low temperatures. Spectral series are shown in Figures 6 and 7, respectively. The two-resonance spectrum of **4A** (Figure 6) at 25 °C begins to broaden below −20 °C. By −80 °C, the spectrum shows two coupled doublets, $^2J_{PNP}$ = 15.9 and 17.1 Hz, in an approximate ratio of 1:1 due to conformers **4Aa** and **4Ab**. Below −90 °C, the low-field resonance (δ = 67) from the PhP(EtNH)– moiety begins to further broaden, perhaps due to the onset of restricted rotation around the PhP(*i*-PrNH)– end of the P–N–P skeleton. Minor impurities, observed as shoulders in the 36.3-MHz $^{31}P\{^1H\}$ spectra, are attributed to traces of the symmetrical *i*-PrN[PhP(EtNH)]$_2$ which has been observed previously but not fully characterized.[20] This impurity appears to be nonintrusive. The spectral series for **7** (Figure 7) begins with an equal-area coupled resonance pattern ($^2J_{PNP}$ = 12.2 Hz) at room temperature which also "freezes" into two sets of coupled doublets, $^2J_{PNP}$ = 12.2 Hz for **7a** and $^2J_{PNP}$ = 20.8 Hz for **7b**.

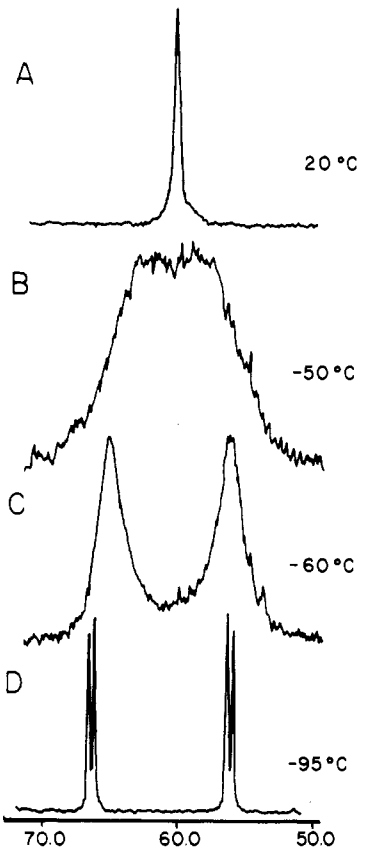

Figure 5. $^{31}P\{^1H\}$ NMR spectra of *meso*-*i*-PrN[PhP(i-PrNH)]$_2$ (**5A**): (A) 20 °C; (B) −50 °C; (C) −60 °C; (D) −95 °C.

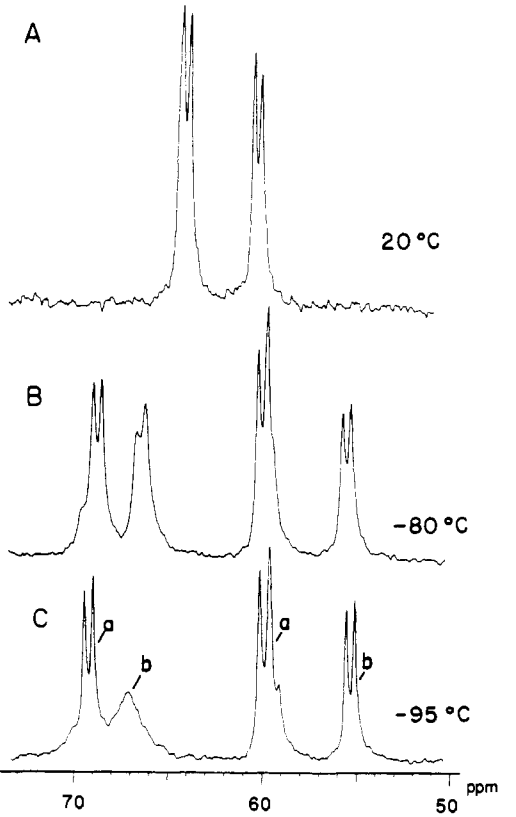

Figure 6. $^{31}P\{^1H\}$ NMR spectra of *erythro*-*i*-PrN[PhP(i-PrNH)][PhP(EtNH)] (**4A**): (A) 20 °C; (B) −80 °C; (C) −95 °C (letters **a** and **b** designate the two conformations observed).

Isomers **7a** and **7b** are present in a 3.5:1 ratio. Two very small doublets at δ 56.3 and 66.2 may be attributable to a third, very

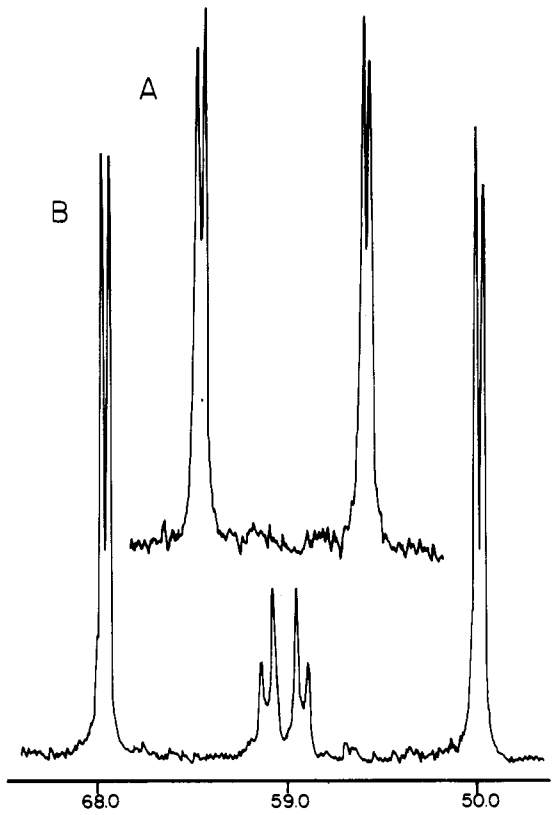

Figure 7. $^{31}P\{^1H\}$ NMR spectra of *erythro*-*i*-PrN[PhP(*i*-PrNH)][PhP(PhNH)] (**7**): (A) 20 °C; (B) −80 °C.

minor (<5%) conformation. The **4Aa**:**4Ab** ratio of 1:1 at low temperature indicates there is very little energy difference between these two conformations.

Several features of the conformational behavior of the bis(phosphino)amines in solution and the relationship of these to the conformations in the solid are noteworthy. (i) All conformations assumed at low temperature have similar $^2J_{PNP}$ coupling constants, in the narrow range of 12.2–20.8 Hz. Earlier workers have suggested that $^2J_{PNP}$ values around P–N–P skeletons depend markedly on conformation; large positive couplings are associated with the *cis* C_{2v} **1B** conformation, and relativley small negative couplings (13–35 Hz) correlate with *trans* **1A** type conformations.[1-6,8-12] Our results seem to confirm this pattern. Assuming that the lowest energy bis(phosphino)amine conformations are those adopted in the solid, we expect the solution "frozen" conformations to be closely similar. As described above, all systems studied were conformationally similar and were of the *trans* **1A** type. (ii) The barriers to rotation around P–N bonds of the P_2N skeletons are suprisingly similar, ranging from 41 to 45 kJ/mol. These values are generally consistent with those measured earlier in other P(III)–N bond containing systems.[6a,30-32] In addition, the barriers to P–N bond rotation are not greatly affected by the R-group identity in the series. (iii) Generally, the ambient temperature $^2J_{PNP}$ values observed for the bis(phosphino)amines are close to the $^2J_{PNP}$ values of the frozen conformers (Table 9). For example, in **6** the $^2J_{PNP}$ at 27 °C is 14.6 Hz, whereas $^2J_{PNP}$ in the frozen conformer is 15.9 Hz. We conclude this means that even though conformation and $^2J_{PNP}$ averaging occurs at ambient temperature, the major conformation in the mixture must be a *trans* **1A** conformation. Either the populations of other conformations with different $^2J_{PNP}$ values must be relatively small or the system contains other conformations which also have small $^2J_{PNP}$ values. In particular, there cannot be much of the *cis* **1B** conformers since the latter are expected to have large, 150–660-Hz, $^2J_{PNP}$ values.[3] (iv) Compounds **4A** and **7** at low temperature exist as two conformations. Both have very similar $^2J_{PNP}$ values, e.g. 15.9 and 12.2 Hz for **7a** and **7b**, indicating they must have closely similar P_2N skeletal conformations of the *trans* **1A** type. Thus, it seems likely that the **a** and **b** type conformers might differ only with respect to the relative orientation of the PhP(NH-*i*-Pr)– and PhP(NHR)– groups; in one form, the PhP(NH*i*-Pr)– lone-pair electrons, the N(2)-*i*-Pr group, and the PhP(NHR)– lone pairs are in a "*trans-cis*" arrangement (**10**); in the other conformation (**11**) the situation

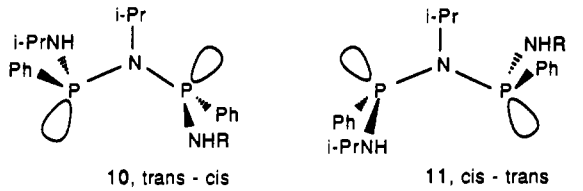

is reversed. Conformations **4Aa** and **4Ab** are closely similar in energy and therefore present in essentially equal populations. However, for **7**, the **7a** form is somewhat favored (**7a**:**7b** = 3.5:1); making **7a** more stable by ca. 2 kJ/mol. Those bis(phosphino)amines of the **4A**, **5A**, **6**, and **7** series which contain the largest R and R′ groups, **5** and **6**, apparently have one distinctly most stable conformation since only one conformer is seen at low temperatures. In contrast, for **4A** and **7**, where the R groups are the smaller Et and Ph groups, conformers of the *trans-cis* and *cis-trans* type (**10** and **11**) appear to be close in energy.

The bis(phosphino)amines described above were all of the *erythro* (or *meso*) type. However, it is also of interest to compare the conformational properties of these major diastereomers to those of the minor *threo* (or *d,l*) diastereomer. Attempts to isolate the *d,l* diastereomer of **5**, **5B**, failed; however, repeated recrystallization of **5A** from a **5A**/**5B** mixture yielded samples enriched in the *d,l* diastereomer, **5B** (**5A**:**5B** = 1:1). The VT $^{31}P\{^1H\}$ NMR data for the **5A**/**5B** mixture are given in Table 9. Two singlet resonances, due to **5A** and **5B**, are seen at 25 °C. Upon cooling, both resonances broaden and eventually split into two equal-area coupled doublets. Resonance pairs at δ 66.2 and 56.2 are assigned to the "frozen" conformer of **5A**, by comparison with the data obtained on pure samples of **5A**, above. Resonances at δ 65.6 and 53.2 are assigned to the analogous conformer from **5B**. The $^2J_{PNP}$ coupling constants are similar, 15.9 and 12.8 Hz for **5A** and **5B**, respectively. In addition, **5A** and **5B** show closely similar coalesence temperatures (T_c = −36 and −40 °C). From these data, P–N bond rotational barriers ($\Delta G^{\ddagger}$) are calculated to be 41.3 and 41.5 kJ/mol for **5A** and **5B**, values that are equal within experimental error. Because of the similarities between the $\Delta G^{\ddagger}$ values, $^2J_{PNP}$ coupling constants, and overall spectral behaviors of **5B** and **5A**, we conclude that **5B**, like **5A**, freezes into an approximate C_s (**1A**) conformation.

The structural data obtained in this study confirms generalizations made earlier[1-20] about how $RN(PXX')_2$ bis(phosphino)amine conformations depend upon the substitutents on the nitrogen (R) and phosphorus atoms (X and X′) of the P–N–P skeleton. Apparently, the steric bulk of both R and X(X′) groups is important, but it appears that the size of the R group might dominate. Most bis(phosphino)amines which have relatively small R groups (H, Me, Et, Ph) are found to have the C_{2v} conformation, **1B**. Even the 1,3,2,4-diazadiphosphetidinyl-containing triphosphazane $[(PhNH)P(NPh)_2P]NPhP(NHPh)_2$[5] and tetraphosphazane $[(PhNH)P(NPh)_2P]_2NPh$,[17] which have relatively large X(X′) groups, assume conformation **1B** in the solid and apparently in solution.[1,6a] Conformation **1B** seems to best minimize the intragroup repulsions among small R, X(X′), and lone pair electrons on the central nitrogen and phosphous atoms. In contrast, conformation **1A** is assumed by bis-

(32) DiStefano, S.; Goldwhite, H.; Mazzola, E. *Org. Magn. Reson.* **1974**, *6*, 1.

(phosphino)amines which have a sterically demanding central R group. Thus, **4A**, **5A**, **6**, and **8** in our work and $RN(PPh_2)_2$ (R = *i*-Pr[1], PPh_2[33]) are all known from X-ray studies to have conformation **1A**. Why the central R group is so important is not clear; however, it is possible that when the R group is large, the intragroup repulsions between R and the X(X′) become dominant and the normally favored conformation **1B** is disfavored relative to **1A**. Conformation **1C** is not seen because in it the repulsions between X(X′) groups on the two PXX′ groups might be too large. Studies to understand further the role of R and X(X′) groups in determining conformation are in progress currently.

Acknowledgment. T.R.P. thanks Dr. L. Luck for help with the DNMR spectral simulation. Support of this work by the National Science Foundation (Grants CHE 8312856 and 8714951) and the Petroleum Research Fund, administered by the American Chemical Society, is gratefully acknowledged.

Supplementary Material Available: Tables of crystal data and refinement details, anisotropic thermal parameters, hydrogen atom positions, nonessential bond distances and angles, and least-squares planes for **4A**, **5A**, and **8** (30 pages). Ordering information is given on any current masthead page.

(33) Ellermann, J.; Köck, E.; Zimmerman, H.; Gomm, M. *Acta Crystallogr.* **1987**, C43.